Available online at www.sciencedirect.com
ScienceDirect
Scripta Materialia 58 (2008) 1086–1089
Scripta MATERIALIA
www.elsevier.com/locate/scriptamat

A dislocation-based model for low-amplitude fatigue behaviour of face-centred cubic single crystals

C. Déprés,[a,*] M. Fivel[b] and L. Tabourot[a]

[a] *Laboratoire SYstèmes et Matériaux pour la MEcatronique, Université de Savoie, BP80439, 74944 Annecy-le-Vieux Cedex, France*
[b] *Laboratoire Science et Ingénierie des MAtériaux et Procédés, Grenoble INP, CNRS, 101 rue de la Physique, BP46, 38402 St Martin D'Hères, France*

Received 20 December 2007; revised 30 January 2008; accepted 2 February 2008
Available online 29 February 2008

A dislocation-based model intended to predict mechanical behaviour for low-amplitude fatigue loading is presented. It is based on a physical representation of the dislocation microstructure according to a statistical distribution of dislocation dipoles acting as efficient obstacles to plastic slip. This leads to a reduced set of equations that accurately predict the development of hysteresis loops during cycling.

Keywords: High-cycle fatigue; Micromechanical modeling; Dislocation dynamics

Most experimental or numerical studies focusing on the description of the dislocation microstructure in face-centred cubic (fcc) single crystals oriented for single slip and subjected to cyclic straining emphasize the same general trends. Dislocations on the primary slip plane multiply and accumulate, forming edge dipoles due to the mutual trapping of opposite sign dislocations. This storage of primary dislocations is often reputed to be heterogeneous, forming networks of edge dislocations commonly referred to as tangles, veins and channels [1,2]. Many authors have drawn inspiration from this general qualitative description to develop so-called two-phase models [3], which exhibit hard phases (containing a high density of dipole areas, which strongly hinder further motion of dislocations) and soft phases (containing a low density of dipole areas) with a characteristic internal length (a dimension comparable to the width of the channel). The existence of such microstructures is a prerequisite of those models, and implies numerous limitations. They only provide a rough approximation of the saturation stress, without giving pertinent information on either the initial cyclic hardening (which is transient in nature) or on the shape of the stress–strain curve during cycling. Because of the lack of proof concerning the existence of well-organized microstructures during the first cycle and of their stability during stress reversal, the dependence of the saturation stress on the existence of well-organized dislocation networks is not obvious [4].

An alternative approach consists of building up a strain-hardening model from the local mechanisms involved during plastic deformation. Following this idea, the strength of dislocation dipoles is expressed as $s = \frac{Gb}{8\pi(1-\nu)h}$, where G and ν are respectively the shear modulus and Poisson ratio, and b is the Burgers vector magnitude. This expression indicates that any dipole of height h acts as an efficient obstacle of strength s to plastic slip. Using this relation, it is shown [1,5,6] that the saturation stress τ_s is inversely related to the average dipole height $\bar{h}$, and that the macroscopic isotropic shear stress is related to the maximal dipole height $h_{\max}$.

In this study, we first propose quantifying the dipole heights, and consequently the dipole strength, from dislocation microstructures computed by a three-dimensional dislocations dynamics (DD) numerical sim- ulation [7]. A grain with a dodecahedric shape oriented for single slip on system $\frac{a}{2}[1\,0\,1](1\,\bar{1}\,\bar{1})$ is cycled 20 times, with an imposed plastic strain amplitude $\Delta\gamma_p = 3 \times 10^{-3}$ (i.e. $-1.5 \times 10^{-3} \leqslant \gamma_p \leqslant +1.5 \times 10^{-3}$). The dislocation microstructure that emerges is planar, and exhibits a dislocation patterning resembling dipolar walls, as shown in Figure 1a. The corresponding analysis of the dipolar height spectrum is shown in Figure 1b. In accordance with transmission electron microscopy observations and measurements in copper [5] or AISI316L stainless steel

* Corresponding author. Tel.: +33 4 50 09 65 62; fax: +33 4 50 09 65 43; e-mail: christophe.depres@univ-savoie.fr

1359-6462/$ - see front matter © 2008 Acta Materialia Inc. Published by Elsevier Ltd. All rights reserved.
doi:10.1016/j.scriptamat.2008.02.027

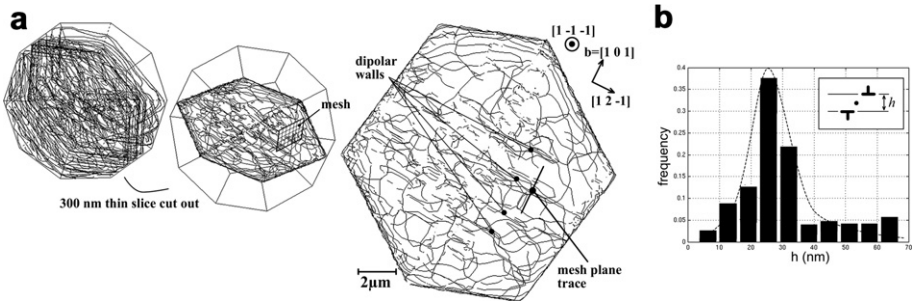

Figure 1. (a) Thin slice (300 nm) cut from a three-dimensional dislocation dynamics simulation of cyclic deformation at $\Delta\gamma_p = 3 \times 10^{-3}$ in a polyedric grain. (b) Statistical distribution of dislocation dipole height.

[6], the dipole height h is random and seems to be normally distributed with an average value $\bar{h}$ that decreases during cycling, namely while dislocation density ρ increases. Moreover, it has been found [6] that $\bar{h}$ is approximately proportional to $\frac{1}{\sqrt{\rho}}$, and that the minimal dipole height $h_{\min}$ remains quite constant (meaning that the standard deviation increases as $\bar{h}$ increases). Since the dipole height h is random, its associated strength s is also a random variable, whose distribution $f(s)$ directly derives from the normal distribution function $\tilde{f}(h)$, according to the relation $f(s) = f(\frac{Gb}{8\pi(1-\nu)h}) = \tilde{f}(h)$.

In the frame of continuum mechanics [8], an appropriate way to numerically represent the dislocation microstructure is to introduce the random variable s and its associated distribution $f(s)$, as an additional state variable to the dislocation density ρ. This formalism implicitly supposes the existence of a representative volume element (RVE), whose dimensions must be chosen to contain enough dislocation dipoles to give a sense to the statistic representation, typically of the order of two or three channels width. Figure 2 shows an example of how function $f(s)$ is built from function $\tilde{f}(h)$, for two given dislocation densities. For more simplicity in this paper, the distribution function $f(s)$ will be assimilated to a normal distribution function. The average value $\bar{s}$ is supposed to be proportional to the dislocation density $\sqrt{\rho}$, to the shear modulus G, and to the magnitude of the Burgers vector b according to the classical relation [9]:

$$\bar{s} = \int_0^\infty s \cdot f(s)\mathrm{d}s = \tau_0 + \alpha G b\sqrt{\rho}, \tag{1}$$

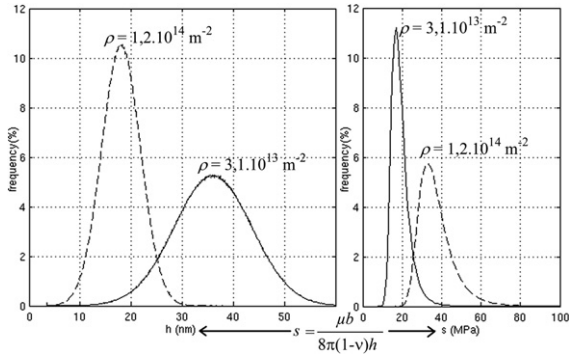

Figure 2. Calculation of the normal distribution of dipole height for two different dislocation densities ($\rho = 3.1 \times 10^{13}$ m^{-2} and $\rho = 1.2 \times 10^{14}$ m^{-2}), and corresponding breaking strength distributions.

where τ_0 is a reference stress. In accordance with DD observations and experimental observations [6,10], the standard deviation σ_s is supposed to be proportional to $\bar{s}$

$$\sigma_s = \sqrt{\int_0^\infty (s-\bar{s})^2 \cdot f(s)\mathrm{d}s} = \lambda \cdot \bar{s}, \tag{2}$$

where the coefficient λ denotes the proportionality coefficient. Clearly, the plastic shear strain rate $\dot{\gamma}$ of the RVE at a given time depends on the state of the dislocation microstructure on the primary system, namely to the distribution $f(s)$. When destabilized under the local resolved shear stress, any dipolar obstacle of strength s is supposed to accommodate the same local shear strain, at a rate $\dot{\gamma}_s$. Since the proportion of obstacles of strength s is $f(s)$, this local strain contributes with a fraction $f(s)\dot{\gamma}_s$ to the global strain rate, leading to the following expression of $\dot{\gamma}$ when the whole s spectrum is taken into account

$$\dot{\gamma} = \int_0^\infty f(s)\dot{\gamma}_s \mathrm{d}s. \tag{3}$$

The flow law governing the local strain rate $\dot{\gamma}_s$ for a given local resolved shear stress is derived from the thermal activation glide theory. It is classically expressed as [11,12]

$$\dot{\gamma}_s = \dot{\gamma}_0 \left|\frac{\tau - X_s}{s}\right|^{1/m} \mathrm{sign}(\tau - X_s).$$

It means that a dipole of strength s will be destabilized provided the local shear stress $(\tau - X_s)$ becomes slightly greater than the temperature-independent breaking strength s of the dipole. In this expression, τ denotes the applied shear stress, X_s the internal long-range stress, and m and $\dot{\gamma}_0$ are respectively a strain rate sensitivity exponent and a reference strain rate, whose dependence on temperature has been established [12].

The main difficulty of the problem is to give an estimate of the long-range stress X_s induced by the surrounding dislocation microstructure on a dipole of strength s. According to many authors [10], the origin of the long-range stress can be understood in terms of strain heterogeneity. Dipoles and dipolar walls indeed contribute to hardening by partially impeding dislocation motion on the primary slip system, leading to shear strain heterogeneity in the primary slip plane. This heterogeneity is evidenced by DD simulations as shown in the deformed mesh plotted in Figure 3a. The grid is centered on a small dipolar wall, perpendicular to the primary slip plane and parallel with the Burgers vector

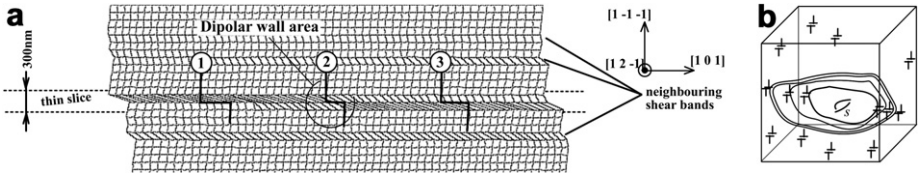

Figure 3. (a) Displacement field of a mesh grid centered around a dipolar wall, located in Figure 1. This illustrates the plastic strain heterogeneity in the thin slice. (b) Schematic representation of the trapping of dislocation loops emitted by a dislocation dipole.

(see the location in Fig. 1a). The mesh is deformed according to the plastic steps induced by the dislocation motion. Displacements of three rows (numbered 1, 2 and 3) of the mesh are highlighted with a bold line. The second row, which intersects the dipolar wall, exhibits a lower shear than rows 1 and 3, which are located in the channels. This difference in shear clearly proves the strain heterogeneity along the slip plane, and directly explains the necessary presence of polarized dislocations between rows 1 and 2 (as well as between rows 2 and 3). These polarized structures behave like "mini pile-ups", which locally store elastic energy inducing a local back-stress acting against the parent dislocation sources. Following this idea, X_s can be estimated from dislocation theory [13]. Consider the scheme in Figure 3b. A dislocation dipole of strength s is centered in a volume of size $2R$, and has emitted n dislocation loops with approximate radius $r_1, r_2, \ldots, r_n$, each one being in equilibrium against some dipolar obstacles. n is directly linked to the strain heterogeneity between the local deformation γ_s around the source dipole and the volume global deformation γ, according to $n = \frac{2R}{b}(\gamma_s - \gamma)$. Assuming that the back stress induced by all the dislocation loops is equivalent to that of a loop of mean radius $\bar{r}$ and Burgers vector nb, this stress can be written as $X_s = n\frac{AGb}{2\bar{r}}$, where A is a parameter depending on the actual shape of the loops. Taking the above expression for n, this gives $X_s = AG\frac{R}{\bar{r}}(\gamma_s - \gamma) = MG(\gamma_s - \gamma)$. In this expression, the coefficient M is somewhat phenomenological since it integrates the mean effect of poorly defined features of the microstructure, such as the actual shape of the polarized loops, and their mean radius relative to the volume dimensions. DD computations yield to an estimate: $M\# 2$. Finally, the complete expression for the flow law is

$$\dot{\gamma}_s = \dot{\gamma}_0 \left| \frac{\tau - MG(\gamma_s - \gamma)}{s} \right|^{1/m} \operatorname{sign}(\tau - MG(\gamma_s - \gamma)). \tag{4}$$

The last law needed to close this set of constitutive equations describes the evolution of the total dislocation density as a function of the strain rate, according to the relation proposed in Refs. [2,11]:

$$\dot{\rho} = \frac{1}{b}\left(\frac{\sqrt{\rho}}{K} - 2y_c\rho\right)|\dot{\gamma}|. \tag{5}$$

This expresses the balance between the accumulation of dislocations after a mean free path K related to the trapping against dipolar obstacles, and annihilation at a rate controlled by the mean distance y_c. The saturation dislocation density ρ_{sat} may be defined as $\rho_{sat} = \frac{1}{4y_c^2K^2}$.

Finally, the low-amplitude fatigue behaviour of a single crystal oriented for single slip is described by a set of only five equations, whose implementation is basic. This model is now tested on pure copper single crystal, for which numerous experimental results are available in the literature. The identification of the parameters has been realized to fit experiments performed at room temperature in Ref. [14]. The optimum values are reported in Table 1. Figure 4 shows the predicted development of the hysteresis loops for a single crystal cycled with a plastic shear strain amplitude $\Delta\gamma_p = 3 \times 10^{-3}$. The

Table 1. Parameters for pure copper at $T = 295$ K

y_c (m)	K	G (GPa)	M	m	$\dot{\gamma}_0$	τ_0 (MPa)	b (Å)	α	λ
2×10^{-9}	35	45	2	0.05	10^{-10}	4	2.56	0.3	0.8

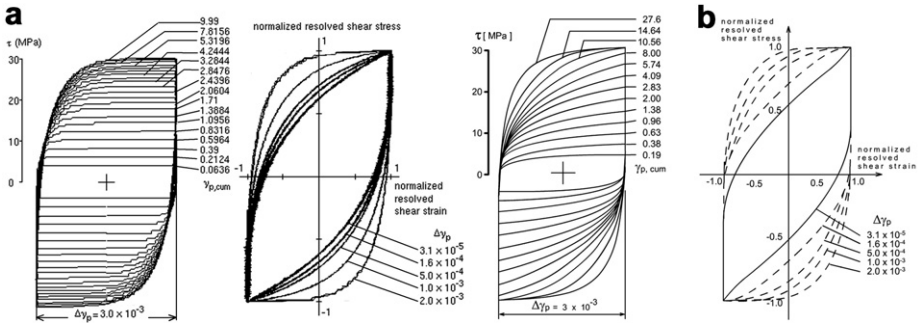

Figure 4. (a) Predicted hysteresis loop evolution during cycling at $\Delta\gamma_p = 3 \times 10^{-3}$ and predicted loop shape as a function of imposed shear strain (given in a normalized format). (b) Corresponding experimental results in copper single crystal [14].

curve is directly compared with experimental measurements [14], and a good agreement can be seen. During the first cycles, the loops do not exhibit real Bauschinger effect, meaning that the back stress $MG(\gamma_s - \gamma)$ is close to zero for any obstacles. The reason is that the microstructural heterogeneity is not yet developed, as mathematically expressed by Eqs. (1) and (2). Indeed, the mean strength of obstacles and their dispersions at the very beginning of the cyclic deformation are small. As cycling proceeds, the dislocation density grows (Eq. (5)), leading to an increase in both the mean obstacle strength and the standard deviation (microstructural heterogeneity). This induces hysteresis loops whose maximal stress is higher, and the Bauschinger effect becomes more pronounced. The saturation loop is reached when the dislocation density reaches the saturation value ρ_{sat}. Parameters y_c and K have been chosen to fit the experimental measurements of the mean dislocation density, classically $\rho_{sat} = 3 \times 10^{14}\ m^{-2}$ [2]. An important feature of fatigue behaviour is the dependence of the shape of the hysteresis loops at saturation on the imposed plastic strain amplitude, as experimentally found in Ref. [14]. Figure 4 compares the shapes of the loops for different plastic strain amplitudes, given in a normalized format. Once again, a good agreement between experiments and prediction is observed.

In Figure 5, the possibilities of the model are tested by plotting the cyclic hardening curves. The computed saturation stress is in good agreement with observations. Note, however, that the slight softening observed for larger strain amplitudes is not reproduced. This could be attributed to the very specific, well-organized substructures (persistent slip bands) observed for such amplitudes which have not been integrated in the proposed theory. Another discrepancy concerns the prediction of the number of cycles to saturation, meaning that the classical production law (Eq. (5)) is not fully valid for cyclic loading path. The reason is that Eq. (5) forces the dislocation density to grow whatever the sign of the strain rate, which is not fully exact. Indeed, DD studies show a slight recovery of the dislocation density during unloading, which is more important when the strain amplitude is low. Further investigations should integrate this aspect.

A few concluding remarks should be made in order to give a better general view of the theoretical formulation described here. (1) The simplified statistical representation of the dislocation microstructure adopted in the present work is a good approximation. Indeed, it only affects slightly the shape of the hysteresis loops. A better representation [6] would increase the loop shape accuracy, but inherently increase the number of governing equations. (2) It is possible to combine Eqs. (1)–(5) to obtain an explicit expression of the hardening law, for a monotonic loading where no evolution of ρ is supposed, and where destabilized dipole strength spreads from 0 to an arbitrary s_{lim}. This expression is:

$$\tau = \int_0^{s_{lim}} f(s) s \mathrm{d}s + MG \frac{1 - \int_0^{s_{lim}} f(s)\mathrm{d}s}{\int_0^{s_{lim}} f(s)\mathrm{d}s} \gamma,$$

meaning that at a given instant, the loading point is given by $\int_0^{s_{lim}} f(s) s \mathrm{d}s$, whereas the hardening modulus is $MG \frac{1-\int_0^{s_{lim}} f(s)\mathrm{d}s}{\int_0^{s_{lim}} f(s)\mathrm{d}s}$. It is instructive to consider two cases. The first one is when a very small proportion of the dipoles are destabilized, namely when $s_{lim} \approx s_{min}$. In this case, the hardening modulus is infinite because $\int_0^{s_{lim}} f(s)\mathrm{d}s \approx 0$. It is precisely what happens just after stress reversal, or for low imposed plastic strain amplitude. The second case is when most of the dipoles are destabilized, namely when $s_{lim} \approx \infty$. The hardening modulus is then zero because $\int_0^{s_{lim}} f(s)\mathrm{d}s \approx 1$, and the loading point is $\bar{s}$. This means that the hardening modulus evolves continuously from infinity to zero, in accordance with observations. Moreover, the stress reaches a saturation value opposed to the mean slip resistance of the microstructure, as commonly expressed in most of the classical dislocation-based models devoted to monotonic loading simulation [11].

The present work, in which the dislocation microstructure is described according to a statistical study, offers an original formulation of a dislocation-based model that is useful for treating mechanical behaviour in low-amplitude fatigue problems. Despite a reduced number of physical equations and parameters, it correctly predicts the development of hysteresis loops in fcc single crystals for different strain amplitudes, from the initial cycle to saturation. Forthcoming works will focus on the implementation of the complete 12 slip systems of the fcc structure, in order to address larger strain amplitudes.

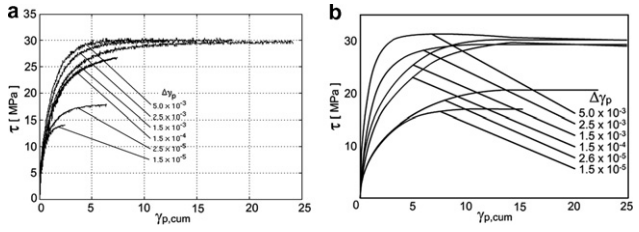

Figure 5. (a) Predicted cyclic hardening curve at different imposed plastic strain. (b) Corresponding experimental results in copper single crystal [14].

[1] S. Suresh, Fatigue of Material, Cambridge University Press, Cambridge, 2001.
[2] U. Essmann, H. Mughrabi, Philos. Mag. 40 (1979) 731.
[3] H. Mughrabi, Acta Metall. 31 (1983) 1367.
[4] C. Gaudin, X. Feaugas, Acta Mater. 52 (2004) 3097.
[5] M.E. Kassner, M.A. Wall, M.A. Delos-Reyes, Mater. Sci. Eng. A 317 (2001) 28.
[6] S. Catalao, X. Feaugas, P. Pilvin, M.-T. Cabrillat, Mater. Sci. Eng. A 400–401 (2005) 349.
[7] C. Depres, C. Robertson, M. Fivel, Philos. Mag. 84 (2004) 2257.
[8] E.A. Repetto, M. Ortiz, Acta Mater. 45 (1997) 2577.
[9] H. Mughrabi, in: A.S. Argon (Ed.), Constitutive Equations in Plasticity, MIT Press, Cambridge, MA, 1975.
[10] X. Feaugas, H. Haddou, Philos. Mag. 87 (2007) 989.
[11] L. Tabourot, M. Fivel, E. Rauch, Mater. Sci. Eng. 234 (1997) 639.
[12] C. Teodosiu, Int. J. Eng. Sci. 23 (1976) 157.
[13] J.P. Hirth, J. Lothe, Theory of Dislocations, Wiley, New York, 1982.
[14] H. Mughrabi, Mater. Sci. Eng. 33 (1978) 207.